RSC Advances

PAPER

View Article Online
View Journal | View Issue

Cite this: *RSC Adv.*, 2023, **13**, 5529

Hyaluronic acid-coated gold nanoparticles as a controlled drug delivery system for poorly water-soluble drugs†

Hyoung-Mi Kim,[a] Jae Hong Park,[a] You Jin Choi,[a] Jae-Min Oh[b] and Junghun Park *[a]

Hyaluronic acid (HA) is a natural linear polysaccharide which has been widely used in cosmetics and pharmaceuticals including drug delivery systems because of its excellent biocompatibility. In this study, we investigated the one-pot synthesis of HA-coated gold nanoparticles (AuNP-HA) as a drug delivery carrier. The HAs with different molecular weights were produced by e-beam irradiation and employed as coating materials for AuNPs. Sulfasalazine (SSZ), a poorly water-soluble drug, was used to demonstrate the efficiency of drug delivery and the controlled release behaviour of the AuNP-HA. As the molecular weight of the HA decreased, the drug encapsulation efficiency of the SSZ increased up to 94%, while drug loading capacity of the SSZ was maintained at the level of about 70%. The prepared AuNP-HA-SSZ exhibited slow release of the SSZ over a short time and excellent sensitivity to different pHs and physiological conditions. The SSZ release rate was the lowest in simulated gastric conditions and the highest in simulated intestinal conditions. In this case, the AuNP-HA protects the SSZ from release under the acidic pH conditions in the stomach; on the other hand, the drug release was facilitated in the basic environment of the small intestine and colon. The SSZ was released under simulated intestinal conditions through anomalous drug transport and followed the Korsmeyer–Peppas model. Therefore, this study suggests that AuNP-HA is a promising orally-administered and intestine-targeted drug delivery system with controlled release characteristics.

Received 16th November 2022
Accepted 9th February 2023

DOI: 10.1039/d2ra07276a

rsc.li/rsc-advances

1. Introduction

Hyaluronic acid (HA) is a biosynthetic natural polymer composed of repeating units of D-glucuronic acid and *N*-acetyl-D-glucosamine disaccharides.[1] It is a representative glycosaminoglycan with essential structural and biological functions in the connective tissue of animal cells. Since HA possesses excellent biocompatible properties,[2,3] it plays an important role in research and has been applied in biomaterials, cosmetics, and pharmaceuticals.[4–7] In particular, pure or modified HA has been widely studied as a supporting material to construct various drug delivery systems involving nanoparticles, liposomes, and microneedle patches to improve drug penetration and stability.[8–10]

In recent years, HA-coated gold nanoparticles (AuNP-HA) have attracted increasing interest for drug delivery and controlled release because of their large surface area, nontoxicity, and chemical inertness.[11–14] In addition, nanoparticles for drug delivery should be small and uniform in order to evade immune system in human body and to facilitate access to the intracellular environment.[15] AuNP can be easily synthesized to be uniform nano-sized drug delivery carriers in the controlled environment. In the case of the HA-based nanoparticles, HA is known to prevent opsonisation by acting as a non-adhesive polymer for most blood proteins and play a role in extending the circulation time of nanoparticles.[16,17] Kumar *et al.* prepared AuNP-HA for metformin delivery, wherein AuNPs were synthesized by using an eggplant extract as a reducing agent and HA was utilized as a capping and targeting agent.[18] Low molecular weight HA (5 kDa) was employed as surface functionalizing material of AuNPs to improve penetration ability of AuNP through the eye barriers and enhances stability of AuNPs in different media and pHs.[19] In addition, small-interfering RNA delivery system by utilizing AuNP-HA was reported for lung cancer treatment.[20]

The AuNP-HA is a promising biocompatible nanomaterial; however, the general synthesis of a AuNP-HA-based drug delivery system requires several chemical reaction steps. The process is unsuitable for scaled-up production as it is time-consuming and causes material loss. To overcome these limitations, one-pot synthesis involving various chemical transformations without purifying the intermediate compounds is

[a]*Biomedical Manufacturing Technology Center (BMTC), Korea Institute of Industrial Technology (KITECH), Yeongcheon-si, Gyeongsangbuk-do 38822, Republic of Korea. E-mail: junghunpark@kitech.re.kr*

[b]*Department of Energy and Materials Engineering, Dongguk University-Seoul, Seoul 04620, Republic of Korea*

† Electronic supplementary information (ESI) available. See DOI: https://doi.org/10.1039/d2ra07276a

promising to reduce the reaction time and to save chemical resources.[21,22] Wang *et al.* reported the synthesis of AuNP-HA-based surface-enhanced Raman spectroscopy probes conjugated with malachite green in a single pot, demonstrating that chemical molecules can be incorporated into AuNP-HA during the one-pot synthesis of nanoparticles. To the best of our knowledge, no study has been conducted to investigate influence of molecular weight of HA for AuNP-HA-based drug delivery system.

In this study, we synthesized AuNP-HA incorporated with a poorly water-soluble drug, sulfasalazine (SSZ), to enhance its bioavailability with controlled release by using the one-pot synthesis strategy. The SSZ is a well-known drug used to treat rheumatoid arthritis, Crohn's disease, and ulcerative colitis. The solubility of SSZ in water is 0.57 μg mL^{-1} since the SSZ is a conjugate of 5-aminosalicylic acid and sulfapyridine, which indicates poorly water-soluble drug.[23,24] Recently, several studies have been reported to deliver SSZ with micro or nanoparticles.[25–27] However, they have drawbacks in initial release rate,[25] long term release,[26] or low encapsulation efficiency[27] and they possess complex synthesis method. To overcome these limitations, we newly suggested the one-pot synthesis of AuNP-HA-SSZ as a controlled drug delivery system illustrated in Scheme 1. For the one-pot synthesis, all components, including gold ions(III), HA, and SSZ were mixed in deionized water (DW), and a reducing agent was applied to the mixture. In addition, to investigate the effects of molecular weight and size of HA on the one-pot synthesis of AuNP-HA and the controlled drug delivery system, HAs with different molecular weights were prepared by electron beam (e-beam) irradiation. E-beam irradiation is one of the HA degradation strategies that does not involve chemical property changes.[28,29] We characterized the e-beam-irradiated HAs and AuNP-HA incorporated with SSZ through physicochemical and image analysis. The drug encapsulation efficiency (DEE) and drug loading capacity (DLC) of the AuNP-HA-SSZ were determined by quantifying the absorption of the supernatant using a UV-vis spectrometer. Finally, *in vitro* drug release patterns of the AuNP-HA-SSZs were investigated in various conditions including simulated body fluids with kinetic modelling of controlled drug release patterns.

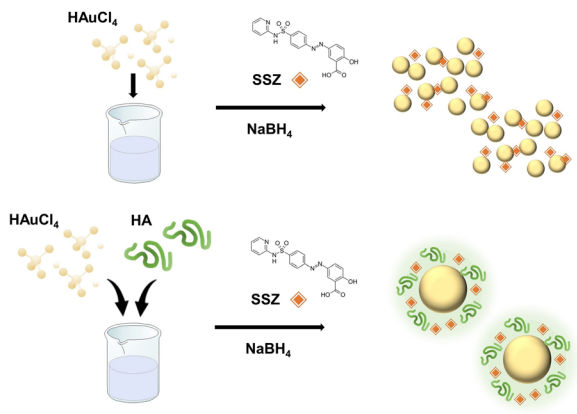

Scheme 1 Schematic illustration for one-pot synthesis of the gold nanoparticle-hyaluronic acid-sulfasalazine (AuNP-HA-SSZ).

2. Materials and methods

2.1. Materials

Medical grade HA powder was purchased from Hyundai Bioland (Lot No. HA022002, Korea). Gold(III) chloride trihydrate ($HAuCl_4$, 99.9%), SSZ, sodium borohydride ($NaBH_4$), sodium chloride, phosphate buffered saline (PBS, pH 7.4), pepsin, hydrochloric acid (1 M), sodium bicarbonate, sodium citrate tribasic dihydrate, and L-ascorbic acid were purchased from Sigma-Aldrich (MO, USA). Dimethyl sulfoxide (DMSO) was purchased from Daejung Chemicals and Metals (Korea). C2C12 cell line (CRL-1772) and fetal bovine serum (FBS, Cat. no. 30-2020) was acquired from American Type Culture Collection (ATCC, USA). Dulbecco's Modified Eagle's Medium (DMEM, Cat. no. SH30243) and penicillin/streptomycin (Cat. no. SV30010) were purchased from Hyclone (USA). Cell counting kit-8 (CCK-8) was purchased from Dojindo Laboratories (Japan).

2.2. E-beam irradiation of HA

The HA powder was dissolved in DW, and the HA solution (22.5 mL, 10 mg mL^{-1}) was placed into a 50 mL conical tube. E-beam irradiation was conducted using a high-frequency linear electron accelerator with an electron energy of 5 MeV and a beam power of 50 kW. The e-beam irradiation dose was adjusted from 1 kGy to 50 kGy by changing the electric current and slat conveyor speed. After irradiation, the HA samples were freeze-dried using a freeze-drier (Advantage Plus EL-85; SP Scientific, USA) for long-term preservation.

2.3. Characterization of e-beam irradiated HA

The polymeric size and exact mass of the e-beam-irradiated HAs were determined by gel permeation chromatography (GPC; 1260 HPLC system, Agilent Technologies, USA) coupled with a multi-angle light scattering (MALS; Dawn Heleos II and Optilab T-rEX, Wyatt Technology Corp., USA) system. Shodex OHpak SB-804 HQ for e-beam-irradiated HAs and OHpak SB-806 HQ (Shodex, Japan) for pristine HA were connected to the GPC with a mobile phase of 0.1 M NaCl (pH 7.0). The separation was conducted by 0.8 mL min^{-1} flow rate at 40 °C column temperature, and 100 μL samples were injected with a concentration of 7 mg mL^{-1}. Data acquisition and analysis were implemented using Astra software v.6.1. The molecular weight analyses were performed in triplicates and displayed mean value with standard derivation. The chemical structure of the HAs was analysed by Fourier transform-infrared spectroscopy (FT-IR; Frontier, PerkinElmer, USA), and the data were analysed using Spectrum v10.5.3. FT-IR spectra were obtained using the conventional attenuated total reflectance mode in the range of 400–4000 cm^{-1}. The dynamic viscosity of the HAs was determined using 5 mg mL^{-1} of each diluted HA using a standard rotary viscometer (WVS-2M, Daihan, Korea) at room temperature. The viscosity analyses were performed in triplicates and displayed mean value with standard derivation.

2.4. One-pot synthesis of AuNP-HA with SSZ

The one-pot synthesis of AuNP-HA was conducted using a previously reported method.[21] In 10 mL of DW, 24 mg of $HAuCl_4$, and 0.4 mg of HA were mixed and stirred for 5 min at room temperature. After mixing, 2 mg $NaBH_4$ was added to the mixture. The mixture was continuously stirred for 24 h until the colour of the solution changed from yellow to red-purple. To synthesize SSZ-incorporated AuNP-HA (AuNP-HA-SSZ), 1 mL of 100 mg mL^{-1} SSZ in DMSO was added to the gold–HA mixture with $NaBH_4$. Thereafter, the precipitate was collected by centrifugation at 17 000 × *g* for 5 min and thoroughly washed with DW. The HA samples were freeze-dried for long-term preservation.

2.5. Characterization of the AuNP-HA-SSZ

The particle size and morphology of the AuNP-HA-SSZ were analysed by transmission electron microscopy (TEM; HT 7700, Hitachi Co., Japan). The particle size distribution was statistically analysed by randomly measuring 100 particles from the TEM images. The histograms of particle diameter were fitted with normal distribution patterns, including kurtosis and skewness factors using Microsoft Excel. The absorption spectra were analysed using a UV-visible spectrometer (UV-vis; BIOMATE 3S, Thermo Fisher Scientific, USA). Hydrodynamic diameters, including zeta potential and polydispersity index (PDI), were obtained with dynamic light scattering (DLS; ELSZ-1000, Otsuka Electronics Co. Ltd., Japan) using properly dispersed and diluted samples in DW.

2.6. Evaluation of DEE and DLC

The nanoparticle suspensions were separated by centrifugation at 17 000 × *g* for 5 min, and the supernatants were collected. The DEE and DLC were evaluated by measuring the absorption intensity of the supernatants on a microplate reader (Synergy H1; BioTek, USA) in the range of 300–700 nm. The DEE and DLC were calculated according to the following equations:[30]

$$\mathrm{DEE}(\%) = \frac{\mathrm{AMT_{total}} - \mathrm{AMT_{free}}}{\mathrm{AMT_{total}}} \times 100 \quad (1)$$

$$\mathrm{DLC}(\%) = \frac{\mathrm{AMT_{total}} - \mathrm{AMT_{free}}}{W_\mathrm{n}} \times 100 \quad (2)$$

where $\mathrm{AMT_{total}}$ is the total input amount of SSZ, $\mathrm{AMT_{free}}$ is the amount of free SSZ in the supernatant (not incorporated), and W_n is the weight of synthesized nanoparticles. All measurements were performed in triplicates, and the mean values with standard deviations were reported.

2.7. SSZ release study

The time-dependent SSZ release profiles were investigated using DW, PBS (pH 7.4), simulated gastric fluid, and simulated intestinal fluid. The two simulated body fluids were prepared by considering the general route of oral administration. We prepared simulated gastric solution by mixing 2.0 g of sodium chloride and 3.2 g of pepsin in DW. The mixed solution was titrated to pH 1.5 with 1 M hydrochloric acid and finally massed up to 1 L.[31,32] For the simulated intestinal fluid, 2.0 g of sodium chloride and 3.2 g of pepsin were dissolved in simulated gastric fluid solution were titrated to pH 6.8 using 1.12 M sodium bicarbonate.[33] In 50 mL of each solution, 10 mg of the nanoparticles were dispersed and incubated at 36.5 °C under gentle shaking in a shaker incubator. After collecting 1 mL of the samples at different time intervals, the samples were centrifuged at 17 000 × *g* for 5 min and filtered using syringe filter. 0.2 mL of collected samples was quantified release amount using a microplate reader at a wavelength of 360 nm. All experiments were performed in triplicates, and the mean values with standard deviations were reported.

2.8. Kinetic models

The time-dependent SSZ release behaviour was analysed using the following kinetic models: first-order, Elovich, parabolic diffusion, and Korsmeyer–Peppas. The first-order equation is as follows:

$$\ln Q_t = \ln Q_\mathrm{e} - kt \quad (3)$$

where Q_t is the amount of drug released at a given time (min), Q_e is the amount of drug released at equilibrium, and k is the first-order rate constant (h^{-1}).[34] The equation of Elovich model is

$$Q_t = a + b \ln t \quad (4)$$

where a is the amount of drug released in the initial phase, and b is the drug release rate.[35] The equation of parabolic diffusion is

$$Q_t = a + K_\mathrm{d} \cdot t^{\frac{1}{2}} \quad (5)$$

where K_d is the drug release rate and a is the release rate constant.[36] The equation of Korsmeyer–Peppas model is

$$Q_t = K_\mathrm{sp} \cdot t^n \quad (6)$$

where K_sp is the initial desorption rate constant and n is the desorption rate coefficient.[37]

2.9. Cytotoxicity assay

In vitro cytotoxicity of the AuNP-HA-SSZ was determined by using C2C12 cell line, a subclone of the mouse myoblast cell line, with CCK-8 assay. For the assay, AuNP and SSZ were prepared as a control, and AuNP-HA(0, 2, 20, and 50 kGy)-SSZ was used for test samples. Each sample was diluted with a concentration of 0.1, 1, 10, 100, 200, and 400 μg mL^{-1} in cell culture medium. DMEM supplemented with 10% FBS and 1% penicillin/streptomycin was used to culture the cells. The cells were incubated at 37 °C under a humidified atmosphere with 5% CO_2. The cells were seeded in 96-well cell culture plates with 5.0×10^3 cells per well and cultured for 24 h. After cell attachment, the cells were cultured with target samples and controls for 24 h. Then, CCK-8 reagent was applied to the cell with a concentration of 1 : 5 (CCK-8 reagent:DMEM medium) and the cells were incubated for 4 h. The absorbance was measured using a microplate reader (Synergy H1, Biotek, USA) at 450 nm

wavelength. Cell viability of C2C12 cells was calculated by the following formula:

$$\text{Cell viability}(\%) = \frac{A_{\text{sample}} - A_{\text{blank}}}{A_{\text{control}} - A_{\text{blank}}} \times 100 \quad (7)$$

where A_{sample} is the 450 nm absorbance of the cells treated with AuNP-HA-SSZ; A_{blank} is the 450 nm absorbance of the blank (DMEM medium and CCK-8 solution); and A_{control} is the 450 nm absorbance of control sample (non-treated). The experiments were conducted by six replicates and data were reported by mean value with standard deviation.

3. Results and discussion

3.1. Characterization of e-beam irradiated HAs

The polymeric sizes of the HA after e-beam irradiation were analysed using GPC as shown in Fig. 1a. In case of the e-beam-irradiated HAs, the results show that the retention time increases as the e-beam irradiation dose of the sample increases. Since the retention time is faster as the size of the sample increases, low-energy-irradiated HA has a smaller polymeric size than the high-energy-irradiated HA. In case of pristine HA, GPC analysis was conducted by using a column different from that of e-beam irradiation HAs; therefore, the exact mass analysis should be required for accurate comparison of the HAs. The exact masses of the HAs were calculated using the GPC coupled with MALS system. As shown in Fig. 1b, the molecular weight decreased from 1360 kDa (pristine) to 4 kDa (50 kGy) with the increase in radiation dose due to HA degradation. Abundant hydroxyl radicals were produced when DW was subjected to e-beam, degrading HA to lower molecular weight. The FT-IR spectra of HA and e-beam-irradiated HA demonstrated no significant changes in the fundamental structure as shown in Fig. 1c. The C=O stretching vibrations at 1655 and 1610 cm^{-1} correspond to the amide and carboxylic acid groups, respectively. The NH group at 1563 and 1320 cm^{-1} (amide), C–O group at 1400 cm^{-1} (acid), C–O–C group at 1150 cm^{-1} (O-bridge), and C–OH group at 1042 cm^{-1} are shown in Table S1.† In Fig. 1d, the viscosity of the e-beam-irradiated HA decreased with increasing radiation dose as a consequence of chain scission of the HA backbone where degradation occurred. It reveals a high correlation between the molecular weight and viscosity of the polymer.[38]

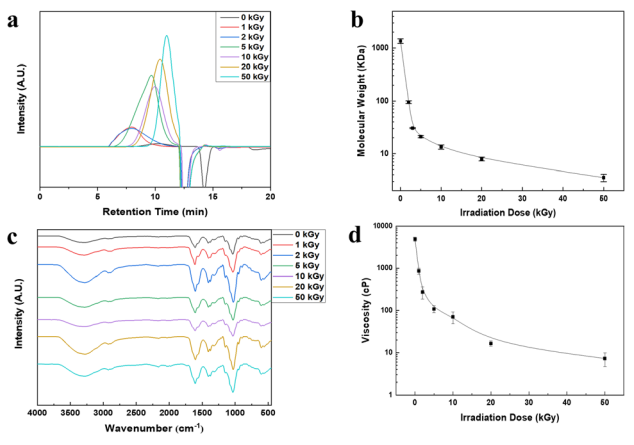

Fig. 1 Characterization results of e-beam-irradiated HAs. (a) GPC profile, (b) molecular weights determined by MALS system, (c) FT-IR spectra with a ranges from 400 cm^{-1} to 4000 cm^{-1}, (d) viscosity of HA solutions. E-beam irradiation doses were 0 (without irradiation), 1, 2, 5, 10, 20, and 50 kGy.

3.2. Characterization of AuNP-HA-SSZ

The SSZ stability was first investigated since the SSZ possesses diazenyl functional group (R–N=N–R′) which can be reduced to sulfapyridine and 5-aminosalicylic acid.[39] In Fig. S1,† UV-vis spectrum of SSZ after the reaction was not changed compared with that of natural SSZ, which demonstrates the SSZ was not chemically affected during the nanoparticle synthesis reaction. Other mild reducing agents, such as sodium citrate or ascorbic acid, were not suitable for the one-pot synthesis of AuNP-HA-SSZ (Fig. S2†). To demonstrate the SSZ-loading capability of the AuNP-HA, four representatives HAs with different molecular weights, *i.e.*, 0 (without irradiation), 2, 20, and 50 kGy-irradiated HAs, were selected for further study. The samples were denoted as AuNP-HA(*X*)-SSZ, where *X* is the e-beam irradiation dose. The

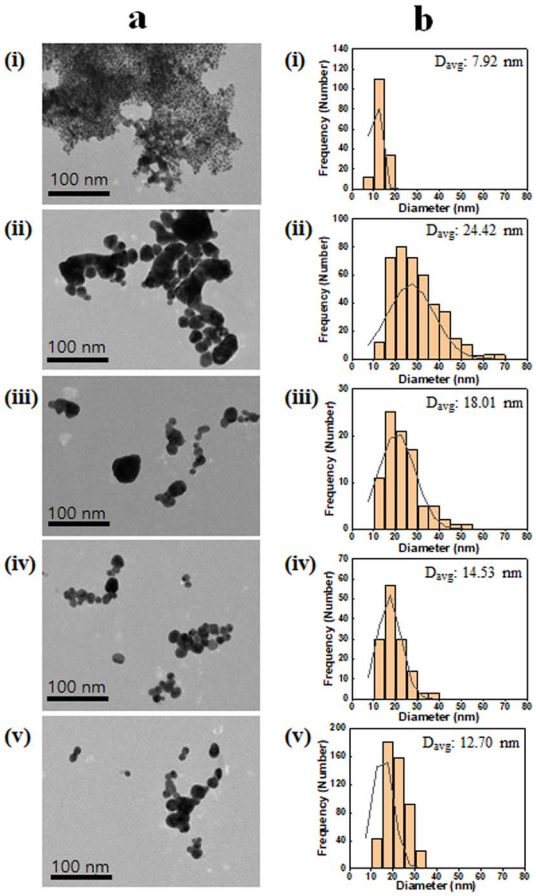

Fig. 2 (a) TEM image of the AuNP-HA-SSZ and (b) size distribution with average diameter of particles (D_{avg}). (i) AuNP-SSZ, (ii) AuNP-HA(0)-SSZ, (iii) AuNP-HA(2 kGy)-SSZ, (iv) AuNP-HA(20 kGy)-SSZ, and (v) AuNP-HA(50 kGy)-SSZ.

morphology and size distribution of AuNP-HA(0)-SSZ, AuNP-HA(2, 20, and 50 kGy)-SSZ, and AuNP-SSZ analysed by TEM images are shown in Fig. 2a. The AuNP-SSZ particle synthesized without HA showed severe aggregation of lots of small particles (Fig. 2a(i)) since any stabilizing agents, generally surfactant, were not applied during the reaction. On the other hand, spherical shape and smooth surface were found for all AuNP-HA-SSZ particles (Fig. 2a(ii)–(v)), which means the HA plays a vital role in stabilizing nanoparticles and preventing aggregation. According to the statistical analyses (Fig. 2b), the average particle diameters of the AuNP-HA(0, 2, 20, and 50 kGy)-SSZ were determined as 24.42, 18.01, 14.53, and 12.70 nm, respectively. In addition, skewness and kurtosis values were evaluated to analyse the size distribution of the synthesized particles (Table S2†). The smaller particles in case of the AuNP-HA(20 and 50 kGy)-SSZ had a narrower distribution than the larger ones, indicating that the particles are uniform in size and shape. In Fig S3,† hydrodynamic diameters of the AuNP-SSZ and the AuNP-HA-SSZs were determined by dynamic light scattering (DLS), which decreased by using low molecular weight HA as the same with TEM image analysis.

The PDI values of the AuNP-SSZ and the AuNP-HA-SSZ are displayed in Fig. 3a. AuNP-SSZ showed a high polydispersity with a PDI value of 1.5, and AuNP-HA(0)-SSZ had a slightly lower PDI value than AuNP-SSZ. In contrast, the PDI values of AuNP-HA(2, 20, and 50 kGy)-SSZ significantly decreased, indicating that the particles prepared with low molecular weight HA were monodisperse. Fig. 3b shows that the zeta potential of AuNP-HA-SSZ was highly negative with a narrow distribution at pH 7.0, confirming that HAs were fully coated on the AuNP surface. It is known that the surface charge plays a very important role in the interaction between nanoparticles and biological substances. The negative surface of AuNP-HA-SSZ would enhance the stability of nanoparticles in systematic circulation.[40] Fig. 3c shows the UV-vis spectra of the nanoparticles. AuNP-HA(50 kGy)-SSZ exhibited a characteristic absorption band at about 540 nm, with a narrow half-peak width. Comparatively, AuNP-HA-SSZ synthesized with higher molecular weight HA showed red-shifted absorption. When AuNP-SSZ was synthesized without HA, the absorption band was broad and weak, indicating that particle aggregation. As a result, low molecular weight HA is favourable for generating more homogeneous AuNP-HA-SSZ particles. Stability of the AuNP-SSZ and the AuNP-HA-SSZs were conducted at various pHs and temperatures (Fig. S4†). The results indicate that physicochemical properties of all samples did not significantly changed under various storage condition.

3.3. DEE and DLC of the AuNP-HA-SSZ

The DEE and DLC of the AuNP-HA-SSZ were investigated by measuring the weights of the input amount of SSZ, free SSZ in supernatants, and finally synthesized nanoparticles. The DEE indicates the amount of drugs incorporated into the synthesized nanoparticles compared with the initial input amount of drugs, and the DLC indicates the mass ratio of drugs to the synthesized nanoparticles.[30] As shown in Fig. 4a, a relatively high DEE value was obtained in the absence of HA, indicating SSZ was adsorbed on the surface of AuNPs due to the increased affinity or interactions between the hydrophobic moieties on SSZ and AuNPs.[41] For the HA-coated AuNPs, more than half of the SSZ was successfully incorporated into the particles. Interestingly, the DEE increased significantly when the molecular weight of HA decreased and reached 96% when 4 kDa HA was used. In the case of low molecular weight HA, since lots of covalent bonds constituting the polymer are decomposed compared to high molecular weight HA, contribution of intermolecular interactions increases over that of covalent bonds when synthesizing the HA layer of the AuNP-HA. Accordingly, SSZ might be more easily incorporated into the HA layer composed of low molecular weight HA, resulting that the DEE increased. On the other hand, DLC values were approximately

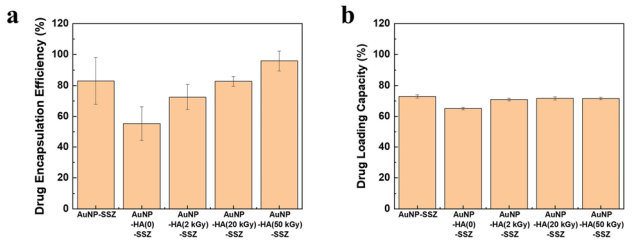

Fig. 4 (a) Drug encapsulation efficiency (DEE) and (b) drug loading capacity (DLC) of the AuNP-SSZ and AuNP-HA-SSZ.

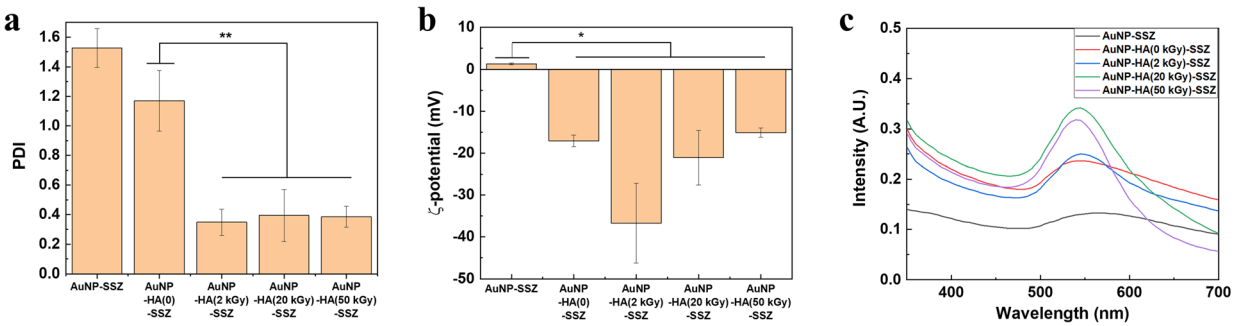

Fig. 3 (a) PDI value and (b) surface charge of AuNP by zeta-potential analysis (*indicates p-value <0.05 and ** indicates p-value <0.01 by Student's t-test). (c) UV-visible spectra of the AuNP-SSZ and AuNP-HA-SSZ.

70% for all AuNP-HA-SSZ particles (Fig. 4b), which indicates a large portion of the synthesized particle mass is occupied by the incorporated SSZ.

3.4. *In vitro* drug release study

The time-dependent release profiles of SSZ in DW and PBS (pH 7.4) are displayed in Fig. 5a and b, respectively. All AuNP-HA-SSZ particles released inconsiderable amounts of SSZ (~7%) in DW within 60 min, and there was no additional release after 60 min. Compared to the dissolution rate of free SSZ in DW, about 47%, the low SSZ release data suggested that SSZ were strongly attached to the AuNP-HA-SSZ particles. In the PBS condition, the SSZ was much more released from AuNP-HA-SSZ particles, over 70% within 5 h, comparable with that of DW condition. To predict the drug release behaviour in the human body, AuNP-HA-SSZ was treated with the simulated gastric fluid and simulated intestinal fluid (Fig. 5c and d) with long-term release of the SSZ (Fig. S5†). The SSZ is an oral administration drug which passes through the stomach in acidic condition and is absorbed in the neutral-weakly basic intestinal condition. The maximum drug release (~95%) occurred in simulated intestinal fluid attributed to its high pH. As the pH increased, the HA matrix began to swell due to the dissolution of carboxylate groups (COO^-), facilitating the release of SSZ from the AuNP-HA. In addition, the HA polymeric layer shielded the encapsulated drug molecules, resulting in sustained release, reducing drug leakage and initial rapid release. Oral absorption of SSZ is affected by the physiological microenvironment. Each part of the digestive system increases from the stomach to the intestine and has a different pH value.[42,43] Drugs may experience several pH-dependent reactions, such as oxidation, hydrolysis, or deamination, which decreased viability.[44] HA generally interferes with drug release under acidic conditions in the stomach and small intestine, and promotes drug release in the high pH environment of the colon, preventing systemic adverse effects and improving therapeutic efficacy.[45]

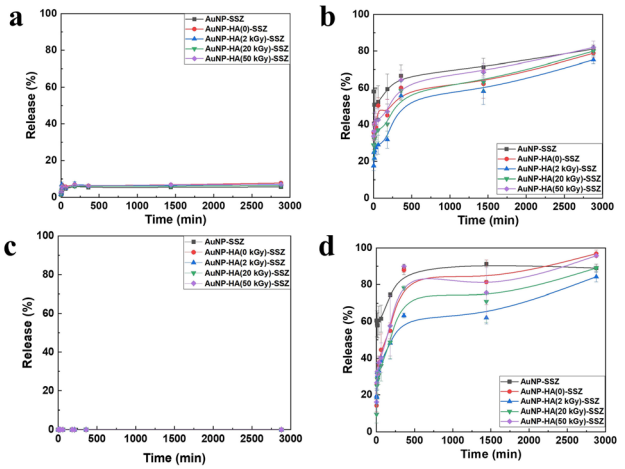

Fig. 5 Time-dependent release patterns of the SSZ from the AuNP-SSZ and the AuNP-HA-SSZ in (a) DW, (b) PBS, (c) simulated gastric solution, and (d) simulated intestinal solution.

3.5. Kinetic modelling of drug release studies

The drug release behaviours of the SSZ from the AuNP-HA-SSZ in PBS and intestinal condition were fitted using various empirical equations based on the nature of the polymer. Kinetic analysis was not conducted for the DW and the simulated gastric solution, since the release patterns were not appropriate for fitting. The empirical equations used for fitting include first order, Elovich, parabolic diffusion, and Korsmeyer–Peppas model, and their regression coefficients (R^2) were calculated (Table 1). The kinetic models imply that the first order model describes the release behaviour mainly by dissolution;[46] the Elovich model explains a release process through bulk surface diffusion;[35,46] parabolic diffusion model is based on ion-exchange phenomena;[36,46] and the Korsmeyer–Peppas model assumes that the release occurs through diffusion from flat surfaces.[37,46] The results show that the Korsmeyer–Peppas equation is considered an appropriate model to describe the SSZ release of the AuNP-HA-SSZ, while in case of the AuNP-SSZ, Elovich model was followed. Therefore, in case of the AuNP-SSZ, the SSZ is released through bulk surface diffusion. On the other hands, in case of AuNP-HA-SSZ, SSZ is released from flat surfaces which implies the SSZ is well incorporated into the particle surfaces. In addition, the experimental release kinetics showed that the drug release did not reach equilibrium in the given time interval. The hydration process was in progress, and the swelling degree did not reach a plateau.[46,47]

The Korsmeyer–Peppas model parameters obtained by fitting are listed in Table 2. The K_{sp} and n values depend on the amounts of loaded drug and the molecular weight of the HA.

Table 1 Regression coefficient (R^2) values of SSZ release pattern from AuNP-HA for kinetic model fitting

Condition	Sample	First order	Elovich	Parabolic diffusion	Korsmeyer–Peppas
PBS	AuNP-SSZ	0.780	0.965	0.560	0.468
	AuNP-HA(0)-SSZ	0.691	0.730	0.942	0.973
	AuNP-HA(2 kGy)-SSZ	0.927	0.700	0.918	0.975
	AuNP-HA(20 kGy)-SSZ	0.945	0.737	0.939	0.956
	AuNP-HA(50 kGy)-SSZ	0.920	0.717	0.948	0.969
Intestinal condition	AuNP-SSZ	0.837	0.908	0.813	0.812
	AuNP-HA(0)-SSZ	0.934	0.962	0.919	0.970
	AuNP-HA(2 kGy)-SSZ	0.742	0.936	0.927	0.980
	AuNP-HA(20 kGy)-SSZ	0.783	0.943	0.938	0.977
	AuNP-HA(50 kGy)-SSZ	0.836	0.796	0.940	0.984

Table 2 Drug release kinetics parameters of AuNP-HA-SSZ in PBS and simulated intestinal solution

Condition	Sample	K_{sp}	n
PBS	AuNP-HA(0)-SSZ	2.924	0.379
	AuNP-HA(2 kGy)-SSZ	2.789	0.457
	AuNP-HA(20 kGy)-SSZ	2.817	0.440
	AuNP-HA(50 kGy)-SSZ	2.818	0.439
Intestinal condition	AuNP-HA(0)-SSZ	3.329	0.514
	AuNP-HA(2 kGy)-SSZ	2.821	0.489
	AuNP-HA(20 kGy)-SSZ	3.129	0.506
	AuNP-HA(50 kGy)-SSZ	3.408	0.513

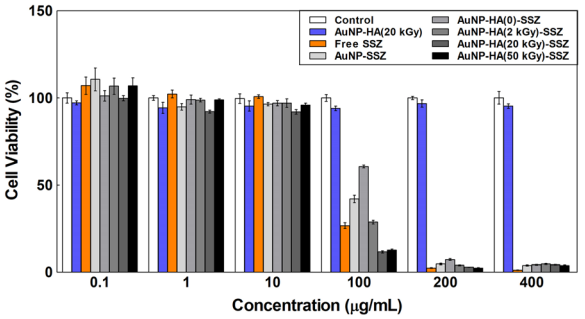

Fig. 6 Cytotoxicity test of the AuNP-HA-SSZ with control samples.

The K_{sp} value provides information about the release rate. A lower K_{sp} indicates a lower drug release rate and a mild interaction between the drug and the carrier.[48] For the PBS condition, there was no significant differences among each samples, while under intestinal conditions, AuNP-HA(50 kGy)-SSZ had a significantly higher K_{sp} value than that of AuNP-HA(2 kGy)-SSZ, suggesting that low molecular weight HA accelerates drug release. The drug release also depends on the diffusion and swelling of the polymer, which represents n value in the Korsmeyer–Peppas model. When $n < 0.43$, the drug release depend on the Fickian diffusion mechanism. The values of $0.43 < n < 0.85$ is considered as non-Fickian drug diffusion mechanism.[49,50] As shown in Table 2, n values were 0.43 to 0.85 (except for AuNP-HA(0)-SSZ in PBS), indicating an anomalous mechanism (non-Fickian) for drug release. It implies that drug diffusion and HA chain relaxation occurred simultaneously to release SSZ. HA swelling facilitates drug dissolution by enhancing the water permeability. Subsequently, the SSZ diffuses from the carrier owing to the chemical potential gradient.

3.6. Cytotoxicity test of the AuNP-HA-SSZ

Biocompatibility of the AuNP-HA-SSZ was investigated by *in vitro* cytotoxicity assay using C2C12 myoblast cell. For the assay, non-treated condition was employed as an assay control, AuNP-HA(20 kGy) and free SSZ was used as control samples. The AuNP-HA-SSZs and the control samples were applied to each well with concentrations from 0.1 μg mL^{-1} to 400 μg mL^{-1} for 24 h. Fig. 6 shows the cell viability results of the AuNP-HA-SSZs with the controls. It can be found that the cell viability of the AuNP-HA(20 kGy) is higher than 90% compared to the assay control even at the highest concentration (400 μg mL^{-1}). In addition, e-beam-irradiated HAs also showed high cell viability (Fig. S6†), demonstrating that the HA and AuNP are biocompatible materials without cytotoxicity. In case of the free SSZ, cytotoxicity to the C2C12 cell was observed by applying over 100 μg mL^{-1} concentration of SSZ. Following the control result, the AuNP-SSZ and AuNP-HA-SSZ also showed cytotoxicity to the C2C12 cell by applying over 100 μg mL^{-1} concentration. Interestingly, as the molecular weight of HA decreased, the cell viability of synthesized nanoparticles decreased at 100 μg mL^{-1} concentration. These results can be interpreted in connection with the drug release pattern. In the case of the AuNP-HA-SSZ using HA with a small molecular weight, it can be understood that the drug release efficiency is high, and thus the cytotoxicity is also high. Therefore, it is confirmed that the AuNP-HA can be used for potential application of drug delivery system with controlled release of drugs.

4. Conclusion

This study reported the one-pot synthesis of the drug-loaded AuNPs assisted by the e-beam irradiated HA. The HA possessing negative charge plays an essential role in well-dispersed nanoparticle synthesis and drug encapsulation. The e-beam irradiation makes low molecular weight HAs without any change of chemical characteristics, and it helps to control nanoparticle morphology and drug encapsulation. The applicability of the AuNP-HA carriers for drug delivery was demonstrated by successful loading of SSZ, poorly water-soluble drug with high levels of the DEE and the DLC. The prepared AuNP-HA-SSZ exhibited a slower release of SSZ over a short time and excellent sensitivity to different pHs and physiological conditions. The drug release was negligible in DW and gastric condition; in contrast, the release rate was the highest in simulated intestinal conditions. The drug release behaviour of the SSZ was fitted using various empirical equations. The results show that the Korsmeyer–Peppas equation is considered an appropriate model to describe SSZ release of the AuNP-HA-SSZ, which indicates the SSZ is released by bulk surface diffusion. In addition, the biocompatibility and efficacy of the AuNP-HA-SSZ was investigated by cytotoxicity test. Therefore, the AuNP-HA demonstrates its potential as an advanced drug delivery carrier with controlled release characteristics.

Author contributions

Hyoung-Mi Kim: conceptualization, methodology, formal analysis, validation, investigation, data curation, writing – original draft; Jae Hong Park: formal analysis, methodology, investigation; You Jin Choi: formal analysis, methodology, investigation; Jae-Min Oh: methodology, investigation, resources, writing – review & editing; Junghun Park: conceptualization, methodology, investigation, resources, writing – review & editing, supervision, funding acquisition.

Conflicts of interest

There are no conflicts to declare.

Acknowledgements

This work was supported by grants from the Korea Institute of Industrial Technology as "Development of fiber-based technology for reduction of hazardous substances in the air (KITECH EO-23-0005)"

References

1 K. Meyer and J. W. Palmer, *J. Biol. Chem.*, 1934, **107**, 629–634.
2 K. Y. Choi, G. Saravanakumar, J. H. Park and K. Park, *Colloids Surf., B*, 2012, **99**, 82–94.
3 L. Zhong, Y. Liu, L. Xu, Q. Li, D. Zhao, Z. Li, H. Zhang, H. Zhang, Q. Kan, J. Sun and Z. He, *Asian J. Pharm. Sci.*, 2019, **14**, 521–530.
4 L. Lapcik Jr, L. Lapcik, S. De Smedt, J. Demeester and P. Chabrecek, *Chem. Rev.*, 1998, **98**, 2663–2684.
5 C. B. Highley, G. D. Prestwich and J. A. Burdick, *Curr. Opin. Biotechnol.*, 2016, **40**, 35–40.
6 S. Li, Q. Dong, X. Peng, Y. Chen, H. Yang, W. Xu, Y. Zhao, P. Xiao and Y. Zhou, *ACS Nano*, 2022, **16**, 11346–11359.
7 Y. W. Zhang, J. Mess, N. Aizarani, P. Mishra, C. Johnson, M. C. Romero-Mulero, J. Rettkowski, K. Schönberger, N. Obier, K. Jäcklein, N. M. Woessner, M.-E. Lalioti, T. Velasco-Hernandez, K. Sikora, R. Wäsch, B. Lehnertz, G. Sauvageau, T. Manke, P. Menendez, S. G. Walter, S. Minguet, E. Laurenti, S. Günther, D. Grün and N. Cabezas-Wallscheid, *Nat. Cell Biol.*, 2022, **24**, 1038–1048.
8 M. Miyazaki, E. Yuba, H. Hayashi, A. Harada and K. Kono, *Bioconjugate Chem.*, 2018, **29**, 44–55.
9 I. S. Bayer, *Molecules*, 2020, **25**, 2649.
10 O. K. Kari, S. Tavakoli, P. Parkkila, S. Baan, R. Savolainen, T. Ruoslahti, N. G. Johansson, J. Ndika, H. Alenius, T. Viitala, A. Urtti and T. Lajunen, *Pharmaceutics*, 2020, **12**, 763.
11 K. Y. Choi, H. S. Han, E. S. Lee, J. M. Shin, B. D. Almquist, D. S. Lee and J. H. Park, *Adv. Mater.*, 2019, **31**, 1803549.
12 T. A. Jacinto, C. F. Rodrigues, A. F. Moreira, S. P. Miguel, E. C. Costa, P. Ferreira and I. J. Correia, *Colloids Surf., B*, 2020, **188**, 110778.
13 C. Mendes, D. P. dos Santos Haupenthal, R. P. Zaccaron, G. de Bem Silveira, M. E. A. B. Corrêa, L. de Roch Casagrande, S. de Sousa Mariano, J. I. de Souza Silva, T. A. M. de Andrade, P. E. Feuser, R. A. Machado-de-Ávila and P. C. L. Silveira, *ACS Biomater. Sci. Eng.*, 2020, **6**, 5132–5144.
14 W. Wei, X. Qi, J. Li, G. Zuo, W. Sheng, J. Zhang and W. Dong, *ACS Biomater. Sci. Eng.*, 2016, **2**, 1386–1394.
15 R. A. Revia, Z. R. Stephen and M. Zhang, *Acc. Chem. Res.*, 2019, **52**, 1496–1506.
16 T. I. Croll, A. J. O'Connor, G. W. Stevens and J. J. Cooper-White, *Biomacromolecules*, 2006, **7**, 1610–1622.
17 A. Almalik, R. Donno, C. J. Cadman, F. Cellesi, P. J. Day and N. Tirelli, *J. Controlled Release*, 2013, **172**, 1142–1150.
18 C. S. Kumar, M. D. Raja, D. S. Sundar, M. Gover Antoniraj and K. Ruckmani, *Carbohydr. Polym.*, 2015, **128**, 63–74.
19 P. S. Apaolaza, M. Busch, E. Asin-Prieto, K. Peynshaert, R. Rathod, K. Remaut, N. Dünker and A. Göpferich, *Exp. Eye Res.*, 2020, **198**, 108151.
20 C.-M. Lin, W.-C. Kao, C.-A. Yeh, H.-J. Chen, S.-Z. Lin, H.-H. Hsieh, W.-S. Sun, C.-H. Chang and H.-S. Hung, *Nanotechnology*, 2015, **26**, 105101.
21 J.-Y. Huang, H.-T. Lin, T.-H. Chen, C.-A. Chen, H.-T. Chang and C.-F. Chen, *ACS Sens.*, 2018, **3**, 174–182.
22 W. Wang, D. Li, Y. Zhang, W. Zhang, P. Ma, X. Wang, D. Song and Y. Sun, *Microchim. Acta*, 2020, **187**, 604.
23 K. T. Savjani, A. K. Gajjar and J. K. Savjani, *ISRN Pharmacol.*, 2012, **2012**, 195727.
24 A. Rajesh, A. Singeeta, H. Lamba, A. Bhandari and K. Sadeep, *Int. Res. J. Pharm.*, 2011, **2**, 200–206.
25 R. Deshmukh, R. K. Harwansh, S. D. Paul and R. Shukla, *J. Drug Deliv. Sci. Technol.*, 2020, **55**, 101495.
26 A. Broesder, S. Y. Bircan, A. B. de Waard, A. C. Eissens, H. W. Frijlink and W. L. J. Hinrichs, *Pharmaceutics*, 2021, **13**, 1985.
27 M.-C. Villa-Hermosilla, A. Fernández-Carballido, C. Hurtado, E. Barcia, C. Montejo, M. Alonso and S. Negro, *Pharmaceutics*, 2021, **13**, 951.
28 J.-i. Choi, J.-K. Kim, J.-H. Kim, D.-K. Kweon and J.-W. Lee, *Carbohydr. Polym.*, 2010, **79**, 1080–1085.
29 M. Tohfafarosh, D. Baykal, J. W. Kiel, K. Mansmann and S. M. Kurtz, *J. Mech. Behav. Biomed. Mater.*, 2016, **53**, 250–256.
30 S. F. Hosseini, M. Zandi, M. Rezaei and F. Farahmandghavi, *Carbohydr. Polym.*, 2013, **95**, 50–56.
31 J. D. Astwood, J. N. Leach and R. L. Fuchs, *Nat. Biotechnol.*, 1996, **14**, 1269–1273.
32 S. H. D. P. Lacerda, J. J. Park, C. Meuse, D. Pristinski, M. L. Becker, A. Karim and J. F. Douglas, *ACS Nano*, 2010, **4**, 365–379.
33 T.-J. Fu, U. R. Abbott and C. Hatzos, *J. Agric. Food Chem.*, 2002, **50**, 7154–7160.
34 J. G. Wagner, *J. Pharm. Sci.*, 1969, **58**, 1253–1257.
35 S. H. Chien and W. R. Clayton, *Soil Sci. Soc. Am. J.*, 1980, **44**, 265–268.
36 D. Steffens and D. L. Sparks, *J. Plant Nutr. Soil Sci.*, 1999, **162**, 599–605.
37 R. W. Korsmeyer, R. Gurny, E. Doelker, P. Buri and N. A. Peppas, *Int. J. Pharm.*, 1983, **15**, 25–35.
38 P. Snetkov, K. Zakharova, S. Morozkina, R. Olekhnovich and M. Uspenskaya, *Polymers*, 2020, **12**, 1800.
39 D. Couto, D. Ribeiro, M. Freitas, A. Gomes, J. L. Lima and E. Fernandes, *Redox Rep.*, 2010, **15**, 259–267.
40 L. Guerrini, R. Alvarez-Puebla and N. Pazos-Perez, *Materials*, 2018, **11**, 1154.
41 K. X. Tan, M. K. Danquah, S. Pan and L. S. Yon, *J. Pharm. Sci.*, 2019, **108**, 2934–2941.
42 E.-M. Collnot, H. Ali and C.-M. Lehr, *J. Controlled Release*, 2012, **161**, 235–246.

43 X. Cai, X. Wang, M. He, Y. Wang, M. Lan, Y. Zhao and F. Gao, *Int. J. Pharm.*, 2021, **606**, 120836.
44 B. Agoram, W. S. Woltosz and M. B. Bolger, *Adv. Drug Delivery Rev.*, 2001, **50**, S41–S67.
45 D. Gugulothu, A. Kulkarni, V. Patravale and P. Dandekar, *J. Pharm. Sci.*, 2014, **103**, 687–696.
46 W. Ajun, S. Yan, G. Li and L. Huili, *Carbohydr. Polym.*, 2009, **75**, 566–574.
47 P. L. Ritger and N. A. Peppas, *J. Controlled Release*, 1987, **5**, 37–42.
48 T. S. Anirudhan, M. M. Anila and S. Franklin, *Mater. Sci. Eng. C*, 2017, **78**, 1125–1134.
49 M. L. Bruschi, *Strategies to modify the drug release from pharmaceutical systems*, Woodhead Publishing, 2015.
50 M. G. Lara, M. V. L. B. Bentley and J. H. Collett, *Int. J. Pharm.*, 2005, **293**, 241–250.